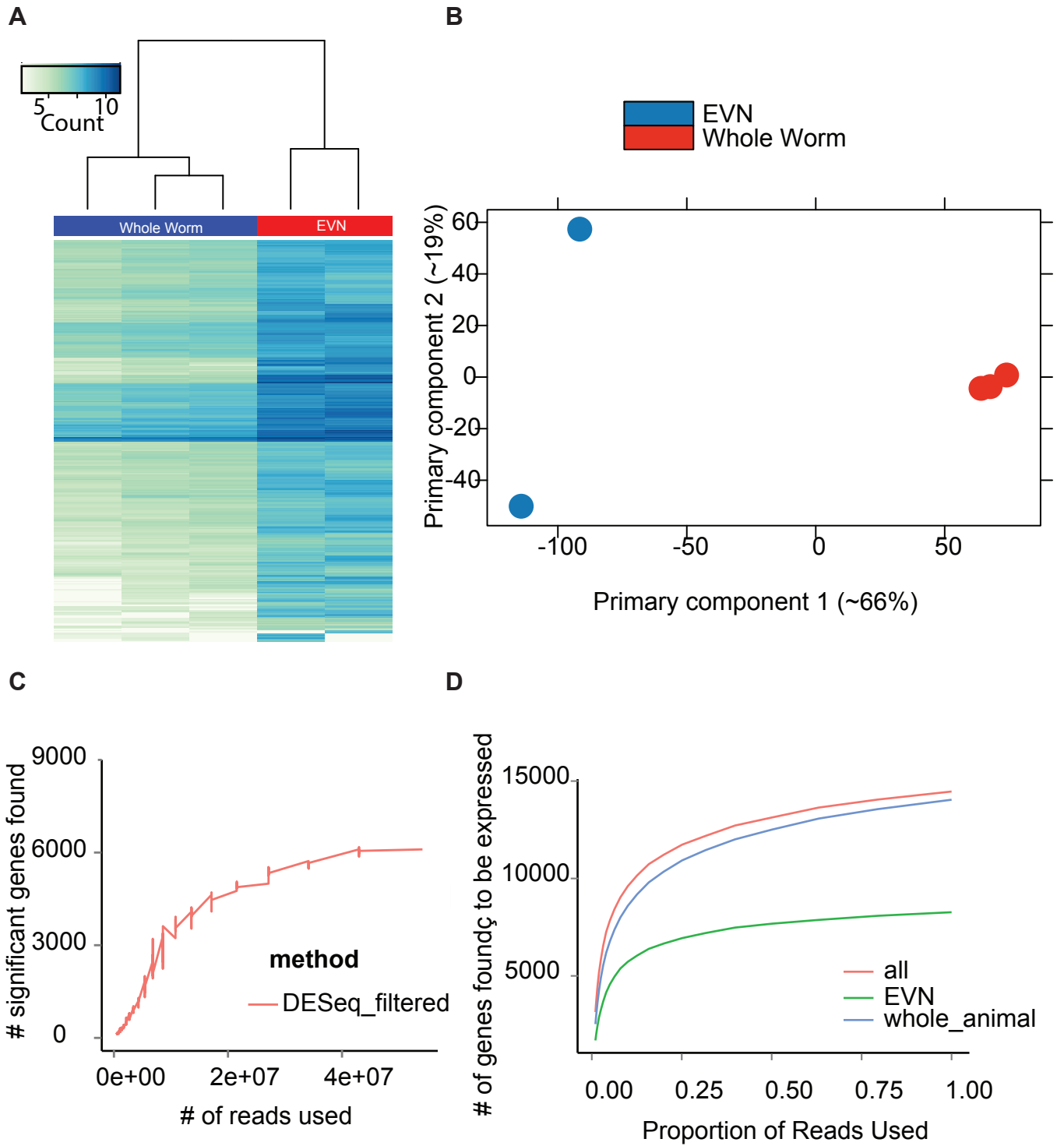


Figure S1



Legends

Supplemental Figure 1, related to Figure 1C-E. (A) Heat map of all 14,464 genes found to be transcribed (>10 reads in at least one of all replicates) in either the whole worm lysates or sorted EVNs. (B) Principal component analysis (PCA) was performed on the normalized, variance stabilization transformed count data using DESeq. The variability captured by the first two principal components (~66% and ~19%) is shown. Isolated EVNs are more variable than the whole worm samples, the main principle component separates the two classes of samples nicely and explains most of the variation in the data. (C) Total reads were downsampled in silico [S1] to the reported proportions ten times and tested for differential expression as described in the text, number of genes found to be significantly differentially expressed (pad < 0.10) are reported on the y-axis. (D) Total reads were downsampled in silico to the reported proportions and tested for expression as described in the text (1/2 of all replicates have > 10 reads), number of genes found to be expressed according to this threshold are reported on the y-axis. From the downsampling, we can see that the number of DEGs we find is mostly saturated even at the depth we're using, not still in the exponential growth phase. There are only 20,000 genes in all of *C. elegans*, so it is not unexpected to detect 70% of these expressed in adult animals. Our data is also consistent with the proportions of whole transcriptome expressed in other more complex animals (mice, humans, etc.)

Table S1, related to Figure 1C-E, Figure 2. The 335 EVN signature genes. Expression pattern were validated by GFP reporter herein (Methods) or in cited publications. Genes that are exclusively expressed in EVNs are in bold. Genes that are expressed in EVNs and other cell types are underlined in bold. No expression indicates our GFP reporter transgenic lines showed no clear expression pattern. Not examined indicates the candidate has not been validated by GFP reporters in this study or other publications.

Table S2, related to Figure 1C-E. Original DEseq data for the differential RNAseq NA, not

available. Table has normalized counts. Per the method of Anders and Huber [S2], transcript count data are normalized, and size factor is calculated to allow the raw count data to then be compared.

Table S3, related to Figure 1. GO Analysis of EVN overrepresented genes. Citations for the programs used are: for GO analysis [S3]; for topGO (topGO: Enrichment analysis for Gene Ontology. R package version 2.22.0.), and the worm annotation package (Carlson M. org.Ce.eg.db: Genome wide annotation for Worm. R package version 3.2.3.). The latter was updated on Oct. 13, 2015. The GO terms are no longer enrichment clusters but are now just the terms unclustered, We used all three annotations (molecular function, biological process, and cell cycle).

Table S4, related to Figure 2, Figure 3, Figure 4 . Several EVN signature genes have predicted or demonstrated function in stress response or innate immunity.

Table S5, related to Figures 3 and 4. Response efficiency (RE) and location efficiency (LE) of mutants corresponding to new EVN signature genes and pathways. n= number of males assayed. Statistical analysis was done by Fisher's exact test, Bonferroni-Holm corrected for RE and one-way ANOVA for LE. Underlined cells are significantly different than wild type (p value indicated in parentheses).

Table S4 Putative immune genes and stress response genes in the EVN signature genes.

Class/gene name	rank	Log2 (klp6p::GFP sorted/unsorted)	P value	Ref
TRAF homologues				
<i>trf-1</i>	29	8.4	<0.001	[S4, S5]
<i>trf-2</i>	30	8.4	<0.001	[S5]
Transcription factors				
<i>daf-19</i>	264	3.3	0.011	[S5]
<i>zip-2</i>	275	3.2	0.011	[S6]
Signaling				
<i>pmk-1</i>	253	3.5	0.029	[S7]
<i>jnk-1</i>	260	3.4	0.038	[S8]
<i>dgk-1</i>	270	3.3	0.040	[S9]
F25B4.2	292	2.9	0.039	[S10]
Detoxifying				
<i>gst-37</i>	32	7.8	<0.001	[S11]
<i>bre-2</i>	106	6.3	0.004	[S12]
<i>gst-28</i>	190	4.3	0.008	[S11]
Stress resistance				
<i>glb-28</i>	74	7.8	0.017	[S13]
<i>pme-4</i>	90	6.9	0.025	[S14]
<i>kin-29</i>	295	2.8	0.023	[S15]
Antimicrobial peptides (AMP)				
F14D7.11	5	10.1	<0.001	[S16, S17]
Y26D4A.5	16	9.3	<0.001	[S16, S17]
F14D7.12	33	7.7	0	[S16, S17]
<i>nlp-1</i>	45	6.5	<0.001	[S18]
F02E11.2	69	8.6	0.047	[S16, S17]
F08G12.8	88	7	0.004	[S16, S17]
Y17G9B.11	128	5.6	0.04	[S16, S17]
R02E12.5	137	5.3	0.028	[S16, S17]
C44B11.4	159	4.8	0.042	[S16, S17]
T23F2.3	196	4.2	0.009	[S16, S17]
<i>fipr-1</i>	203	4.1	0.021	[S19]
K07D4.9	204	4.1	0.019	[S16, S17]
F09E5.16	221	3.9	0.044	[S16, S17]
C type lectin				
<i>cllec-179</i>	8	9.8	<0.001	[S20]
<i>cllec-164</i>	12	9.5	<0.001	[S20]
<i>cllec-113</i>	38	7.4	0.001	[S20]

<i>clec-254</i>	59	Inf	0.002	[S20]
<i>clec-256</i>	62	Inf	0.011	[S20]
<i>clec-255</i>	64	9.3	0.028	[S20]
<i>clec-188</i>	67	9.1	0.015	[S20]
<i>clec-176</i>	75	8.2	0.002	[S20]
<i>clec-251</i>	78	7.8	0.001	[S20]
<i>clec-114</i>	104	6.4	0.002	[S20]
<i>clec-194</i>	105	6.4	0.002	[S20]
<i>clec-112</i>	109	6.3	0.005	[S20]
<i>clec-250</i>	201	4.1	0.045	[S20]
<i>Galectin</i>				
<i>lec-9</i>	292	2.7	0.047	[S20]
MIP-T3 domain				
M01A8.2	274	3.2	0.016	[S21]
S/T rich Mucin like domain				
C35A11.3	2	10.6	<0.001	[S22]
F26C11.3	4	10.3	<0.001	[S22]
F59A6.3	10	9.8	<0.001	[S22]
F49C5.7	21	8.8	<0.001	[S22]
Y53G8AL.3	66	9.2	0.001	[S22]
ZC204.6	83	7.5	0.013	[S22]

Bold genes were validated by GFP reporters that are exclusively expressed in EVNs (Figures 2, 3).

Supplemental Table 5. Mating behavior of candidate gene mutants.

Genotype	Encoding protein Domains/homology	RE (%) (n)	LE (%) (n)
wild type		98.4 ± 2.8 (184)	88.6 ± 1.7 (168)
<i>pkd-2(sy606)</i>	TRPP	15.2 ± 2.2(264)	27.4 ± 3.1 (10)
<i>asic-2(ok289)</i>	DEG/ENaC	93.3 ± 2.9 (75)	81.8 ± 3.0 (66)
<i>cllec-164(gk335531)</i>	C-Lectin	96.0 ± 2.8 (50)	82.9 ± 3.5 (42)
<i>egas-1(ok3497)</i>	DEG/ENaC	97.8 ± 1.6 (90)	72.5 ± 3.4 (82)
F26C11.3(gk453581)	CCP+Mucin like	76.7 ± 6.5 (43)	<u>54.9 ± 8.3 (16) (* p<0.001)</u>
F28A12.3(tm6038)	TGFβ receptor	96.6 ± 2.4 (59)	79.9 ± 3.9 (49)
F31F7.2(WBVar00272087)	vWA	94.6 ± 3.8 (37)	<u>61.8 ± 4.4 (35) (* p<0.001)</u>
F59A6.3(gk643207)	C-Lectin	100 ± 0 (25)	<u>54.9 ± 6.2 (25) (* p<0.001)</u>
<i>nsy-1(ok593)</i>	MAPKKK	83.9 ± 6.7 (31)	88.7 ± 4.9 (28)
<i>sek-1(km4)</i>	MAPKK	93.5 ± 3.7 (46)	86.5 ± 4.6 (43)
<i>tir-1(tm3036)</i>	TIR domain adaptor	85.4 ± 5.6 (41)	75.2 ± 6.3 (36)
F25D7.5(tm4326);pkd-2(sy606)	C-Lectin+5TM	14.6 ± 5.6 (41)	50.0 ± 18.0 (4)
Y70G10A.2(gk183679)	C-Lectin+5TM	97.5 ± 2.5 (40)	84.6 ± 4.9 (39)

* Statistically different from wild type. F25D7.5(tm4326);pkd-2(sy606) is statistically different from wild type but not pkd-2(sy606)

Supplemental Experimental Procedures

C. elegans maintenance

All nematodes were grown under standard conditions [S23]. The strain PT2519: *myIs13* [*P*_{*klp-6*}::*gfp* + *pBX* (plasmid *pha-1(+)*); *him-5*(*e1490*) *V* was used for adult cell isolation.

Adult EVN isolation was performed as described by [S24]. The integrated transgene *myIs13*[*P*_{*klp-6*}::*gfp* + *pBX*] was used to mark EVNs; the *him-5* (*e1490*) mutation was used to generate a male enriched population. Eggs were collected by bleaching adult worms and plated on to HGM (High Growth Media; Same as NGM, except Bacto-peptone 20 g/L, cholesterol 20 mg/L, agar 30 g/L) plates to produce synchronized male-enriched worm cultures. Three plates of synchronized worms on HGM plates were used for each cell sorting. Worms were washed off of plates with M9 buffer (42 mM Na₂HPO₄, 22 mM KH₂PO₄, 86 mM NaCl, 1 mM MgSO₄·7H₂O), put into 1.5ml centrifuge tubes, and washed five more times in M9, until all of the bacterial food was removed. All centrifugation steps were performed in a standard mini-centrifuge (Fisher, max speed: 6000 rpm) for 5 seconds. The worms were then washed once in 500 µl lysis buffer (200 mM DTT, 0.25% SDS, 20 mM HEPES pH 8.0, 3% sucrose) at room temperature (RT). 750ul lysis buffer was added to each tube; animals were incubated at room temperature for exactly 6.5 min. The worms were again washed five times in M9 buffer and spun down. Then, 250 ul of freshly made Pronase (20 mg/mL in ddH₂O; from *Streptomyces griseus*; Sigma-Aldrich Cat No: P6911-1G) was added, and the worm pellet was incubated for 20 min at RT. The worm solution was pipetted vigorously with a P200 tip for 100 times every 5 min to release EVNs; a 2µl sample of worms was examined on a dissecting scope after every pipetting stage to assess the level of dissociation. PBS solution with 2% FBS (Fetal Bovine Serum, Certified, Heat-Inactivated, Invitrogen Cat No: 10082-139) was used to pre-wet a 5 µm syringe filter, which was stored on ice. The dissociated cells were taken up into a 1 mL syringe through a 27 gauge needle before fitting the cooled filter onto the syringe to gently filter cells into a FACS tube on ice. 1 mL PBS solution was used to wash the filter again to recover any remaining cells. The cells then were kept on ice and in darkness until sorting. Cells were sorted using FACSVantage SE w/DiVa (BD Biosciences) directly into 850ul Trizol LS; 150ul sorted cells were added (about

250,000 cells maximum) per tube. Unfiltered cells were used for whole worm cell RNAseq controls.

RNAseq

RNA isolation was according to the protocol for linear amplification microarrays [S25]. RNA-seq, computational analysis and significant gene list generation and transcript identification and abundance analysis (DEseq) was performed as described in [S24]. In brief total reads were downsampled in silico to the reported proportions and tested for expression and differential expression as described in the text. Refer also to Supplemental Figure 1 legend.

GFP reporter construction and transgenic worm generation: Promoter and translational GFP reporters were created using the PCR fusion technique [S26]. A promoter region is chosen according to the following criteria: if intergenic region upstream of start codon is larger than 2 Kb, then 2 Kb sequence upstream of start codon of the gene was used; if the intergenic region upstream of the start codon is smaller than 2 Kb, the whole intergenic region upstream of the start codon was used. For all translational reporters, promoter plus the genomic coding region was fused to GFP coding sequence. 200 ng/μL PCR product of reporter were mixed with 50 ng/μl of pBX and injected into PS2172: *pha-1(e1213ts)III; him-5(e1490)V*.

Mating behavior assays: Response and vulva location assays were modified from [S27]. Briefly, a mating assay lawn was prepared by dropping 13 μl of OP50 *Escherichia coli* bacterial culture in LB broth onto a fresh NGM plate and allowed to dry covered overnight, making a circular lawn of ~ 0.5 cm diameter. Ten minutes prior to the assay, 20 hermaphrodites were scattered onto the mating dot and allowed to acclimate. Male mating behavior was assayed blind as follows: 5 males of the first genotype were released in the center of the mating lawn and observed for 4 minute time period. Response was scored positive when a male touched a hermaphrodite with its tail and began backward scanning of the hermaphrodite. Location of vulva efficiency was

scored by 1 divided by the number of times a male contacted the hermaphrodite vulva until stopping at the vulva. Leaving assays are described in [S28]. Each male genotype was assayed at least three times on separate days to compensate for behavioral variability and to ensure robustness of the results. CB1490: *him-5(e1490)V* males were used as positive wild-type controls, and PT9: *pkd-2(sy606)IV; him-5(e1490)V* males were used as negative controls.

EV release quantification and imaging: Strain PT621 *him-5(e1490) myls4 [PKD-2::GFP +P_{unc-122::gfp}]*V was used as wild type. Both late L4 males and adult males were examined for EV release according to [S29]. Worms were imaged using a Zeiss Axioplan 2 microscope with a 100x 1.4NA oil Zeiss Plan-APOCHROMA objective and Photometrics Cascade 512B EMCCD (Roper Scientific) camera or Zeiss 510 laser scanning confocal microscope. Young adult males were synchronized by picking L4 larvae one day before imaging. Late L4 males with developed fan and rays just before molting were picked from a population of L4 males and imaged within 1-5 hours. Worms were anesthetized with 10 mM levamisole solution, transferred to 2% agarose mounting slides and imaged within 30 minutes of mounting.

Transmission electron microscopy

Young adult nematodes were prepared by high pressure freezing and freeze substitution following described protocols described [S30]. Principal fixation involved 1% osmium, 3% dH₂O in acetone. Serial thick sections were collected onto Pioloform-coated slot grids and examined using a Technai F20 electron microscope. Serial section dual axis electron tomograms were produced from consecutive semi-thick sections (200 nm) using markerless alignment and internal back projection methods, followed by mergers of electron tomograms from consecutive sections [S31].

Strain list

Strain	Genotype	REF
CB1490	<i>him-5(e1490)V</i>	[S32]
PT9	<i>pkd-2(sy606)IV; him-5(e1490)V</i>	[S33]
PT2915	<i>pmk-1(km25)IV; him-5(e1490), myls4(PKD-2::GFP+unc-122p::GFP)V</i>	This study
PT2951	<i>pmk-1(km25)IV; him-5(e1490)V</i>	This study
PT621	<i>him-5(e1490), myls4V</i>	[S34]
PT2946	<i>tir-1(tm3036) III; him-5(e1490)V; myls1(PKD-2::GFP+unc-122p::GFP)IV</i>	This study
PT2947	<i>nsy-1(ok593) II; him-5(e1490)V; myls1</i>	This study
PT2948	<i>him-5(e1490)V; sek-1(km4) X; myls1</i>	This study
PT2949	<i>nsy-1(ok593) II; him-5(e1490)V</i>	This study
PT2950	<i>him-5(e1490)V; sek-1(km4) X</i>	This study
PT2376	<i>trf-1(nr2014)III;him-5(e1490)V</i>	This study

PT2393	<i>trf-1(nr2014), pha-1(e2123)III; him-5(e1490)V; myEx750 (TRF-1::GFP+</i>	This study
PT1722	<i>pha-1(e2123) III; him-5(e1490) V; myEx632[Pklp-6::tdTomato + pBX1]</i>	This study
PT2395	<i>pha-1(e2123)III; him-5(e1490)V; myEx750, myEx632</i>	This study
PT9	<i>pkd-2 (sy606)IV;him-5(e1490)V</i>	This study
PS3401	<i>lov-1(sy582)II;him-5(e1490)V</i>	[S27]
PT2411	<i>trf-1(nr2014)III;pkd-2(sy606)IV;him-5(e1490)V</i>	This study
PT2412	<i>lov-1(sy582)II;trf-1(nr2014)III;him-5(e1490)V</i>	This study
PT2413	<i>lov-1(sy582)II;trf-1(nr2014)III;pkd-2(sy606)IV;him-5(e1490)V</i>	This study
PT2414	<i>tol-1(nr2033)I;him-5(e1490)V</i>	This study
PT2415	<i>ikb-1(nr2027)I;him-5(e1490)V</i>	This study
PT443	<i>pkd-2(sy606)VI;him-5(e1490);myls1</i>	This study
PT2394	<i>trf-1(nr2014)III;pkd-2(sy606)VI;him-5(e1490);myls1</i>	This study
PT2864	<i>pha-1(e2123) III; him-5(e1490) V; myEx865[GLB-28::GFP+ pBX1]</i>	This study
PT2882	<i>pha-1(e2123) III; him-5(e1490)V; myEx869[F26C11.3::GFP+ pBX1]</i>	This study
PT2753	<i>pha-1(e2123) III; him-5(e1490) V; myEx841[C35A11.3p:GFP]+pBX1]</i>	This study
PT2945	<i>pha-1(e2123) III; him-5(e1490) V; myEx877[F25D7.5::GFP+pBX1]</i>	This study
PT2871	<i>pha-1(e2123) III; him-5(e1490) V; myEx858[T09D9.3::GFP+pBX1]</i>	This study
PT2879	<i>pha-1(e2123) III; him-5(e1490) V; myEx866[TF49C5.12::GFP+pBX1]</i>	This study
PT2461	<i>him-5(e1490)V; myEx732[F28A12.3p::GFP,elt-2::mCherry]</i>	This study
PT2862	<i>pha-1(e2123) III; him-5(e1490) V;myEx855[T13F3.7p::G]+Pklp-6::tdTomato</i>	This study
PT2872	<i>pha-1(e2123) III; him-5(e1490) V; myEx859[C18F10.2::GFP+pBX1]</i>	This study
PT2859	<i>pha-1(e2123) III; him-5(e1490) V; myEx859[C18F10.2::GFP+pBX1]</i>	This study
PT2889	<i>pha-1(e2123) III; him-5(e1490) V; myEx874[T06D8.2::GFP+pBX1]</i>	This study
PT2971	<i>pha-1(e2123) III; him-5(e1490) V; myEx876[F14D7.11::GFP+pBX1]</i>	This study
PT2751	<i>pha-1(e2123) III; him-5(e1490) V; myEx839[egas-1p::GFP+pBX1]</i>	This study

PT2757	<i>pha-1(e2123) III; him-5(e1490) V; myEx845[F59A6.3::GFP+pBX1]</i>	This study
PT2860	<i>pha-1(e2123) III; him-5(e1490) V; myEx853[Y70G10A.2::GFP+pBX1]</i>	This study
PT2564	<i>pha-1(e2123) III; him-5(e1490) V; myEx840[ASIC-2::GFP+ pBX1]</i>	This study
PT2875	<i>pha-1(e2123) III; him-5(e1490) V; myEx862[CLEC-164::GFP+pBX1]</i>	This study
PT2944	<i>pha-1(e2123) III; him-5(e1490) V; myEx878[clec-179p::GFP+pBX1]</i>	This study
PT2901	<i>clec-164(gk335531) IV; him-5(e1490) V</i>	This study
PT2902	<i>clec-164(gk335531) IV; him-5(e1490), myls4 V</i>	This study
PT2894	<i>F25D7.5(tm4326)I; pkd-2(sy606)IV; him-5(e1490)V</i>	This study
PT2895	<i>F25D7.5(tm4326)I; pkd-2(sy606), myls1IV; him-5(e1490)V</i>	This study
PT2912	<i>F59A6.3(gk643207)II; pkd-2(sy606), myls1IV; him-5(e1490)V</i>	This study
PT2913	<i>F59A6.3(gk643207)II; him-5(e1490)V</i>	This study
PT2914	<i>F26C11.3(gk453581)II; him-5(e1490)V</i>	This study
PT2900	<i>F26C11.3(gk453581)II; pkd-2(sy606), myls1IV; him-5(e1490)V</i>	This study
PT2761	<i>asic-2(ok289) I; myls13[klp-6p::GFP + pBX1] III; him-5(e1490) V</i>	This study
PT2898	<i>Y70G10A.2(gk183679)III; him-5(e1490)V</i>	This study
PT2899	<i>Y70G10A.2(gk183679)III; pkd-2(sy606), myls1IV; him-5(e1490)V</i>	This study
PT2732	<i>pkd-2(sy606), him-8(e1489)IV, myls1; egas-1(ok3497)V</i>	This study
PT2867	<i>mys13III; egas-1(ok3497)V</i>	This study

Supplemental References

- S1. Robinson, D.G., and Storey, J.D. (2014). subSeq: determining appropriate sequencing depth through efficient read subsampling. *Bioinformatics* *30*, 3424-3426.
- S2. Anders, S., and Huber, W. (2010). Differential expression analysis for sequence count data. *Genome Biol* *11*, R106.
- S3. Alexa, A., Rahnenfuhrer, J., and Lengauer, T. (2006). Improved scoring of functional groups from gene expression data by decorrelating GO graph structure. *Bioinformatics* *22*, 1600-1607.
- S4. Pujol, N., Bonnerot, C., Ewbank, J.J., Kohara, Y., and Thierry-Mieg, D. (2001). The *Caenorhabditis elegans* unc-32 gene encodes alternative forms of a vacuolar ATPase a subunit. *J Biol Chem* *276*, 11913-11921.
- S5. Xie, P. (2013). TRAF molecules in cell signaling and in human diseases. *J Mol Signal* *8*, 7.
- S6. Estes, K.A., Dunbar, T.L., Powell, J.R., Ausubel, F.M., and Troemel, E.R. (2010). bZIP transcription factor zip-2 mediates an early response to *Pseudomonas aeruginosa* infection in *Caenorhabditis elegans*. *Proc Natl Acad Sci U S A* *107*, 2153-2158.
- S7. Aballay, A., Drenkard, E., Hilbun, L.R., and Ausubel, F.M. (2003). *Caenorhabditis elegans* Innate Immune Response Triggered by *Salmonella enterica* Requires Intact LPS and Is Mediated by a MAPK Signaling Pathway. *Curr Biol* *13*, 47-52.
- S8. Oh, S.W., Mukhopadhyay, A., Svrzikapa, N., Jiang, F., Davis, R.J., and Tissenbaum, H.A. (2005). JNK regulates lifespan in *Caenorhabditis elegans* by modulating nuclear translocation of forkhead transcription factor/DAF-16. *Proc Natl Acad Sci U S A* *102*, 4494-4499.
- S9. Kao, C.Y., Los, F.C., and Aroian, R.V. (2008). Nervous about immunity: neuronal signals control innate immune system. *Nat Immunol* *9*, 1329-1330.
- S10. Nicholas, H.R., and Hodgkin, J. (2004). Responses to infection and possible recognition strategies in the innate immune system of *Caenorhabditis elegans*. *Mol Immunol* *41*, 479-493.
- S11. Hasegawa, K., Miwa, S., Isomura, K., Tsutsumiuchi, K., Taniguchi, H., and Miwa, J. (2008). Acrylamide-responsive genes in the nematode *Caenorhabditis elegans*. *Toxicol Sci* *101*, 215-225.
- S12. Marroquin, L.D., Elyassnia, D., Griffiths, J.S., Feitelson, J.S., and Aroian, R.V. (2000). *Bacillus thuringiensis* (Bt) toxin susceptibility and isolation of resistance mutants in the nematode *Caenorhabditis elegans*. *Genetics* *155*, 1693-1699.
- S13. Tilleman, L., Germani, F., De Henau, S., Geuens, E., Hoogewijs, D., Braeckman, B.P., Vanfleteren, J.R., Moens, L., and Dewilde, S. (2011). Globins in *Caenorhabditis elegans*. *IUBMB Life* *63*, 166-174.
- S14. St-Laurent, J.F., Gagnon, S.N., Dequen, F., Hardy, I., and Desnoyers, S. (2007). Altered DNA damage response in *Caenorhabditis elegans* with impaired poly(ADP-ribose) glycohydrolases genes expression. *DNA Repair (Amst)* *6*, 329-343.
- S15. Lanjuin, A., and Sengupta, P. (2002). Regulation of chemosensory receptor expression and sensory signaling by the KIN-29 Ser/Thr kinase. *Neuron* *33*, 369-381.
- S16. Thomas, S., Karnik, S., Barai, R.S., Jayaraman, V.K., and Idicula-Thomas, S. (2010). CAMP: a useful resource for research on antimicrobial peptides. *Nucleic Acids Res* *38*, D774-780.

- S17. Waghu, F.H., Gopi, L., Barai, R.S., Ramteke, P., Nizami, B., and Idicula-Thomas, S. (2014). CAMP: Collection of sequences and structures of antimicrobial peptides. *Nucleic Acids Res* 42, D1154-1158.
- S18. Ren, M., Feng, H., Fu, Y., Land, M., and Rubin, C.S. (2009). Protein kinase D is an essential regulator of *C. elegans* innate immunity. *Immunity* 30, 521-532.
- S19. Pujol, N., Davis, P.A., and Ewbank, J.J. (2012). The Origin and Function of Anti-Fungal Peptides in *C. elegans*: Open Questions. *Front Immunol* 3, 237.
- S20. Schulenburg, H., Hoepfner, M.P., Weiner, J., 3rd, and Bornberg-Bauer, E. (2008). Specificity of the innate immune system and diversity of C-type lectin domain (CTLN) proteins in the nematode *Caenorhabditis elegans*. *Immunobiology* 213, 237-250.
- S21. Ling, L., and Goeddel, D.V. (2000). MIP-T3, a novel protein linking tumor necrosis factor receptor-associated factor 3 to the microtubule network. *J Biol Chem* 275, 23852-23860.
- S22. Lieleg, O., Lieleg, C., Bloom, J., Buck, C.B., and Ribbeck, K. (2012). Mucin biopolymers as broad-spectrum antiviral agents. *Biomacromolecules* 13, 1724-1732.
- S23. Brenner, S. (1974). The genetics of *Caenorhabditis elegans*. *Genetics* 77, 71-94.
- S24. Kaletsky, R., Williams, A.B., Arey, R., Lakhina, V., Landis, J.L., and Murphy, C.T. (in review). Transcriptional profiling of isolated adult *C. elegans* neurons identifies the neuronal IIS/FOXO transcriptome and a new regulator of axon regeneration.
- S25. Murphy, C.T., McCarroll, S.A., Bargmann, C.I., Fraser, A., Kamath, R.S., Ahringer, J., Li, H., and Kenyon, C. (2003). Genes that act downstream of DAF-16 to influence the lifespan of *Caenorhabditis elegans*. *Nature* 424, 277-283.
- S26. Hobert, O. (2002). PCR fusion-based approach to create reporter gene constructs for expression analysis in transgenic *C. elegans*. *Biotechniques* 32, 728-730.
- S27. Barr, M.M., and Sternberg, P.W. (1999). A polycystic kidney-disease gene homologue required for male mating behaviour in *C. elegans*. *Nature* 401, 386-389.
- S28. Lipton, J., Kleemann, G., Ghosh, R., Lints, R., and Emmons, S.W. (2004). Mate searching in *Caenorhabditis elegans*: a genetic model for sex drive in a simple invertebrate. *J Neurosci* 24, 7427-7434.
- S29. Wang, J., Silva, M., Haas, L.A., Morsci, N.S., Nguyen, K.C., Hall, D.H., and Barr, M.M. (2014). *C. elegans* Ciliated Sensory Neurons Release Extracellular Vesicles that Function in Animal Communication. *Curr Biol* 24, 519-525.
- S30. Hall, D.H., Hartwig, E., and Nguyen, K.C. (2012). Modern electron microscopy methods for *C. elegans*. *Methods Cell Biol* 107, 93-149.
- S31. Hall, D.H., and Rice, W.J. (2015). Electron tomography methods for *C. elegans*. In *C. elegans, Methods and Applications*, Volume in press, G. Haspel and D. Biron, eds. (Humana Press).
- S32. Hodgkin, J. (1983). Male phenotypes and mating efficiency in *Caenorhabditis elegans*. *Genetics* 103, 43-64.
- S33. Barr, M.M., DeModena, J., Braun, D., Nguyen, C.Q., Hall, D.H., and Sternberg, P.W. (2001). The *Caenorhabditis elegans* autosomal dominant polycystic kidney disease gene homologs *lov-1* and *pkd-2* act in the same pathway. *Curr Biol* 11, 1341-1346.
- S34. Bae, Y.K., Lyman-Gingerich, J., Barr, M.M., and Knobel, K.M. (2008). Identification of genes involved in the ciliary trafficking of *C. elegans* PKD-2. *Dev Dyn* 237, 2021-2029.

